A laboratory study on the effects of waves on the performance and structural deflection of a tidal stream turbine

Stuart Walker, Lorenzo Cappietti, Irene Simonetti

Abstract— **An experimental study was carried out to determine the effect of waves on a horizontal axis tidal turbine, from both power-generation and structural perspectives. Hindcast and recorded wave and tidal flow data for two locations (one in the Messina Strait in the Mediterranean Sea, the other in the Sound of Islay in the North Atlantic) was used to establish scale sample flow, under which a 1:81 scale turbine was tested in the LABIMA wave-current flume at the University of Florence. A 1:81 scale turbine model based on commercial turbine geometry was instrumented to record power output and forces acting on the support structure.**

Flow cases included waves of varying height and period, and flow cases ranging from benign to extreme. Waves arriving from both upstream and downstream were studied.

We found that when simulating a real case of 1.3m/s flow velocity, the presence of large and long period waves (5.7m with 10.8s period) actually improved the total turbine power generation over a 25-second period. This was not the case in faster flow rate cases, when waves were detrimental to overall turbine power output. We also found that the presence of waves dramatically increase the forces applied to the turbine support structure.

Keywords—**Power generation, Structural effects, Tidal Turbine, Waves.**

I. Introduction

OCEANS are hostile environments for engineered structures. Though similar to oil and gas and offshore wind structures, tidal turbines have unique characteristics, and the effect of a lifetime in this environment is currently not well understood. Such an understanding is crucial to the efficient and cost-effective design of tidal turbines, and will become increasingly so as the industry moves from a demonstration to full commercial phase.

Environments in which tidal turbines are likely to be installed (commonly channels between landmass) are often subject to highly energetic waves, which impact the performance of the turbine by altering the flow profile reaching the turbine blades, and also impact the structural loading on the turbine support structure.

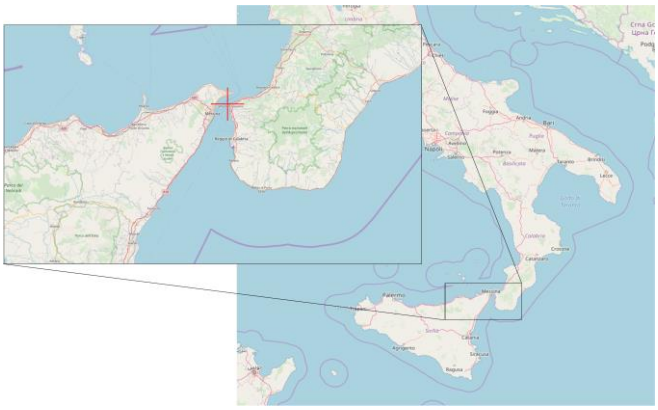

Fig. 1. Location of the Mediterranean site selected for experimental replication in this study. The location chosen (indicated by the red cross) lies in the centre of the Messina Strait at latitude 38.23°N and longitude 15.62°E.

Previous studies proved that the presence of waves may affect both the turbine power output and thrust [1], [2] and the structural loading [3], [4] however the effect of waves on the performance of a tidal turbine is, at present, not sufficiently well understood, particularly regarding the case of waves opposing the current.

This study thus aimed to test a scale model of a horizontal axis tidal turbine under the effect of realistic combinations of flow and wave cases and to record the impact on turbine performance and structural deflection of the support structure, also considering the case of waves opposing the current direction.

This paper is structured as follows: the procedure adopted to develop the realistic test cases and the description of the experimental test set-up are presented first. Laboratory results are then analysed, discussing the effect of waves on both the turbine power output and the structural deflection.

Paper ID: 1501, Tidal Device Development and Testing.

This work was supported by Marinet2, and the University of Sheffield Department of Applied Inkjet Printing.

S. Walker is at the Institute for Innovation in Sustainable Engineering, University of Derby, Lonsdale House, DE1 3HD (e-mail: s.walker2@derby.ac.uk).

L. Cappietti and I. Simonetti are at LABIMA, Università degli Studi di Firenze, Via Santa Marta 3, 50139, Florence, Italy (email: l.cappietti@unifi.it, irene.simonetti@unifi.it).

A. *Locations*

Two real sites were used to generate the input data for this study, one in the Messina Strait (MS) in the Mediterranean Sea, and one in the Sound of Islay (SI) in the North Atlantic. To generate realistic site data, we first selected feasible tidal turbine installation locations. These locations were chosen as they represent the extremes of potential tidal location sites. While tidal velocities at both sites are sufficient to make the sites potentially suitable for economic power extraction, the North Atlantic is a very energetic site, while the Mediterranean site is in a generally calmer location.

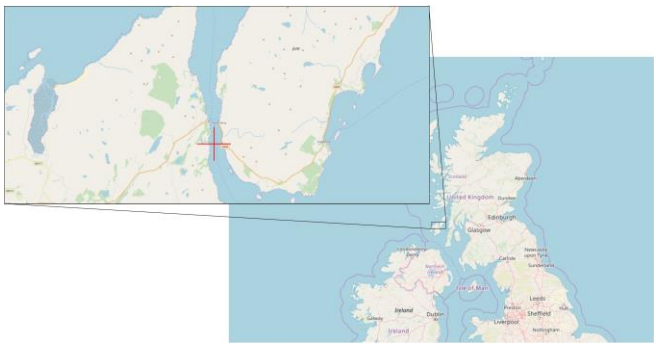

Fig. 2. Location of the North Atlantic site selected for experimental replication in this study. The location chosen (indicated by the red cross) lies in the centre of the Sound of Islay at latitude 55.85°N and longitude 6.10°W

The Messina Strait is a 5km wide channel between the Italian mainland and the island of Sicily, at the meeting of the Ionian Sea to the south and the Tyrrhenian Sea to the north, and is perhaps one of the most suitable sites for tidal power generation in the Mediterranean. The deepest point of the channel is 250m deep, and tidal velocities reach 2.5m/s [5]. Fig. 1 shows the location of the strait and the location used in this study.

Maximum ebb and flow values in the Messina Strait occur at different locations [6], so the location with the greatest mean absolute value of flow velocity was selected.

The selected location is at a latitude of 38.23°N and longitude 15.62°E.

The Sound of Islay is a channel between the islands of Islay and Jura, off the west coast of Scotland. The channel is approximately 1km wide, and 198m deep at its deepest point. The channel is known for high tidal velocities, with a maximum of around 3.7m/s. In 2010 this location was confirmed as the site of the ScottishPower Renewables Sound of Islay Demonstration Tidal Array [7]. The location selected for use in this study lies at latitude 55.85°N and longitude of 6.10°W. Fig. 2 shows the location used in this study.

II. MATERIAL AND METHODS

The project described here comprised two main sections: the development of a series of condition cases from hindcast data for the selected sites, and the laboratory testing of scale turbine models under these conditions.

B. *Development of test cases*

Having selected the locations to be replicated in our testing, tidal flow velocity and wave conditions were required. Both recorded and hindcast data was used (hindcast data describes data generated for a historical time period, using a statistical model, itself based on recorded data). Data from EMODnet [8] was used to provide bathymetric conditions and aid the scaling of the experiments. Tidal flow velocity conditions were classified using data from the Copernicus Marine Environment Monitoring Service [9],[10] at the Messina Strait (MS) and Sound of Islay (SI) sites. This data was recorded at a frequency of 30 minutes for the full year of 2017.

Wave data for the MS case was taken from the Alghero wave bouy installed as part of the Italian Wave Network [11]. Though this location is in a different location (West of Sardinia Island), work on the Wavewatch III model [12] suggests that this location experiences similar conditions to the Messina Strait. The Italian Wave Network buoy data was recorded for a 30-minute period at a three hour frequency between 1/7/1989 and 31/12/2007. This gives a much greater temporal resolution than is available at the MS site.

Wave data for the SI case was taken from the DHI MetOcean Data Portal [13]. Data was recorded by the NASA Jason-1 satellite with temporal resolution of around 2 seconds. Data recorded between 15/3/2016 and 15/3/2017 was used in this study.

At the MS and SI locations, data from these sources was classified to give three values of each variable (tidal velocity, wave height, wave period), classified as benign, moderate and extreme. The cases were extracted from the data by taking the 80^{th}, 90^{th} and 95^{th} percentiles respectively.

Wave period data in each case was also required, and was taken as the mean wave period at each of the height cases, for example the benign wave period was taken as the mean period of all instances of the defined benign wave height.

It was found that benign and moderate conditions in the SI case corresponded almost exactly to moderate and extreme MS cases, thus giving four separate cases across the two sites. These cases are shown in Table 1.

Fig. 3. Turbulence generating structures (l) and wave absorbing structure (r) installed in the LABIMA wave-current flume.

The resulting case scenarios were then scaled to the water channel size and used to establish test cases during the experimental campaign.

TABLE I
TIDAL VELOCITY, WAVE HEIGHT AND WAVE PERIOD CASES FROM FULL-SCALE SITE DATA

Flow case:	F1+ / F4*	F2+ / F5*	F3+ / F6*	F7+ / F8*
MS:	Benign	Moderate	Extreme	-
SI:	-	Benign	Moderate	Extreme
Flow speed (m/s)	0.8	1.3	1.7	2.1
Wave period (s)	7.2	9.0	10.8	15.3
Wave height (m)	2.4	4.0	5.7	8.9

+upstream flow conditions(current – waves in the same direction)
**downstream flow conditions (current-wave in opposite directions)*

An experimental scale factor of 1:81 (s=*81*) was used. Froude scaling was applied, meaning a factor of s was used to calculate scale water depth, turbine sizing and wave height, and a factor of $s^{0.5}$ was used to scale flow velocity and wave period. In order to replicate a 17.5m blade diameter turbine in 25m water depth, a turbine model of blade diameter 216mm and a channel water depth of 300mm were used. The four flow velocity cases in Table 1 (0.8m/s, 1.3m/s, 1.7m/s and 2.1m/s) translate to water channel mean velocities of 0.1m/s, 0.14m/s, 0.19m/s and 0.23 m/s respectively.

Next, we developed the wave cases by combining height and period cases taken from the site data. Eight combination wave cases were developed:

- MS benign wave height and period (H1)
- MS moderate (SI benign) wave height and period (H2)
- MS extreme (SI moderate) wave height and period (H3)
- MS moderate wave height with MS benign period (H4)
- MS moderate wave height with MS extreme period (H5)
- MS extreme wave height with MS benign period (H9)
- MS extreme wave height with MS moderate period (H10)

The cases replicated experimentally are shown in Table 2, both at real scale and channel scale. As suggested by the case numbering, further cases were developed and tested, but their analysis is not included in this article (e.g. SI extreme wave height and period and SI moderate wave height with SI extreme period).

C. *Test Facility*

The Wave-Current Flume at LABIMA, University of Florence, is 37m in length and 800mm wide. A water depth of 300mm was used for all tests in this study. A recirculating pump is installed in a pipe manifold of 250mm diameter and controlled by a frequency modulating controller (model Danfoss VLT). The wave maker is a bespoke AM3 system capable of producing

Fig. 4. SPECuWaTT project scale turbine model.

waves of up to 0.35m height and of periods greater than 8s. Wave height were measured using ultrasonic wave gauges (model Honeywell 943-F4V-2D-1C0-330E). Four such gauges were used, installed at approximately one third and two thirds of the distance across the channel (250mm from the channel walls in each case), at 420mm upstream and 430mm downstream of the turbine installation location. Flow rate was measured by a magnetic flow meter (model Danfoss MAGFLO MAG3100W). The scaled velocities described in the previous section (Table 1) give bulk flow rates through the channel of 25l/s, 37.5l/s, 50l/s and 62.5l/s.

It is well known that the upstream turbulence intensity plays a key role in the response of horizontal axis turbine, and it may affect both blade loading and power extraction [14], [15], [16]. For this reason, prior to testing, the channel was characterised in order to capture flow profiles and turbulence data for the cases to be tested. Profiles were captured using a Nortek Vectrino Acoustic Doppler Velocimeter at the turbine installation location for each of the wave and flow cases subsequently used to test the turbine. During characterisation it was noted that the turbulence intensity of the empty channel was much lower than that expected of a real tidal installation site, and (in common with many other experimental studies) turbulence-generating structures would be required.

The location of the wave-making equipment is fixed, so in order to facilitate the eventual testing of cases with wave propagation and tidal flow in the same direction, and cases with wave propagation opposing tidal flow, it was necessary to simulate tidal flow from both ends of the channel. Consequently, turbulence-generating structures were installed both upstream and downstream of the turbine. A combination of blocks and mesh were used. Cubic stone blocks of 120mm width were installed with a cross-channel separation distance of 150mm and a streamwise separation distance of 200mm between rows.

Alternating rows of two and three blocks were used, covering a total distance of 2.4m between 6.6m and 9.0m downstream of the turbine installation location. A stainless steel mesh of 12mm grid size was installed across the channel and over its full depth, at a distance of 5.4m up and downstream of the turbine installation location. An absorbing structure was added to the channel to diffuse wave power and reduce reflection from the end of the channel. This perforated steel structure was 2.4m in length and reached across the channel, angled upwards from the base to above the height of the highest waves to be tested. The turbulence-generating blocks and absorbing structure used are illustrated in Fig. 3.

For the four flow velocity cases described in Table 1, mean streamwise turbulent intensities for cases without waves were 1.3%, 6.2%, 4.9%, and 8.2% (details on the procedure adopted to calculate turbulent intensity from measured data can be found in [17]). The addition of benign case waves increased turbulent intensity values to between 5% for low flow rate and 15% for high flow rate cases. This compares to turbulence intensity of 12-13% recorded experimentally at a site with maximum flow velocity of 2.5m/s [18]. Turbulent intensity of over 30% was seen in some extreme wave cases.

D. Turbine Model

The turbine model used in this study was a three-blade horizontal axis turbine, representative of most commercial tidal turbine concepts. The blade profile was based on that of a commercial design and was manufactured in polyacrylate at the University of Sheffield Department of Applied Inkjet Printing. The turbine blades each measure 100mm from root to tip, with a 12° degree root-tip twist, a tip chord of 8mm and a root chord of 26mm. The blades were mounted on a nacelle, which was itself fixed to the turbine generator. No gearbox or other power transfer mechanisms were used. The support structure of the turbine was a simple 8mm diameter post design without a complex support base, tripod or other fixing arrangement. This design was chosen to allow the measurement of structural deflection on a homogeneous support structure. The turbine and support structure were mounted on a steel base of 200mm x 200mm and 7mm thickness, designed to hold the turbine in position without a requirement to fix it to the base of the channel. The support structure was 117mm in length from the base to the generator, meaning that the centre of the nacelle was 137mm above the channel base. The turbine is shown in Figure 4.

1) Turbine Instrumentation

In order to measure performance and structural deflection, the turbine model was equipped with a generator and strain gauges. A small DC motor (model MFA RE-385) was used as a generator. The voltage produced by the generator was measured using the LABIMA Data Acquisition system. Since the key performance output of the turbine in this study is the relative power generation, generator output was not scaled or calibrated to rotational speed. Instead, generator voltage was used to give a direct comparison between cases.

We installed copper foil strain gauges (model BF350, 350Ω with sensitivity coefficient 2.1) on the turbine support structure at a height of 58.5mm above the base of the support structure. One gauge was installed on the upstream-facing portion of the support structure, and another perpendicular to this on the side of the support structure. Gauges were installed in a half-bridge configuration, and were supplied with 5V via the LABIMA data acquisition system and deflection recorded using the same system.

2) Strain Gauge calibration

In order to correlate support structure deflection and strain gauge voltage output, the gauges were calibrated using a load cell (model AEP transducers Type FJ). A rigid steel bar was fixed between the load cell and the centre of the nacelle, and the turbine was incrementally moved towards the load cell whilst recording both strain gauge and load cell outputs. Testing was repeated multiple times and were found to be unaffected by the direction of movement of the structure (i.e. whether the turbine was moving towards or away from the load cell). We observed a linear relationship between the deflection of the structure and the load applied, with a slope of 0.59N/mV.

E. Test procedure

For each test, the following procedure was carried out: Flow conditions were set by adjusting the motor controller to a predetermined frequency to give the required flow rate for each velocity (as defined in Section C). A period of time was allowed to ensure stable flow conditions, then the test was started. LABIMA uses a combined wave generation and data acquisition system and all measurement equipment was routed through this system, resulting in a single output file for each test. Each test began with a 10 second period without waves, followed by a 30 second period of wave generation, followed by a 30 second period without wave generation. In some cases

TABLE II
HEIGHT AND PERIOD OF FULL SCALE AND CHANNEL SCALE SIMULATED WAVE CASES

	Real scale		Channel scale	
Case	Height (m)	Period (s)	Height (m)	Period (s)
H1	2.4	7.2	0.03	0.8
H2	4.0	9.0	0.05	1.0
H3	5.7	10.8	0.07	1.2
H4	4.0	7.2	0.05	0.8
H5	4.0	10.8	0.05	1.2
H9	5.7	7.2	0.07	0.8
H10	5.7	9.0	0.07	1.0

where flow direction opposed wave propagation direction it was found that the 30 second period was insufficient to allow the waves to reach the turbine. In these cases, the wave generation time period was extended to 60 seconds. An acquisition frequency of 200 Hz was used for the ultrasonic wave gauge and for the strain gauges.

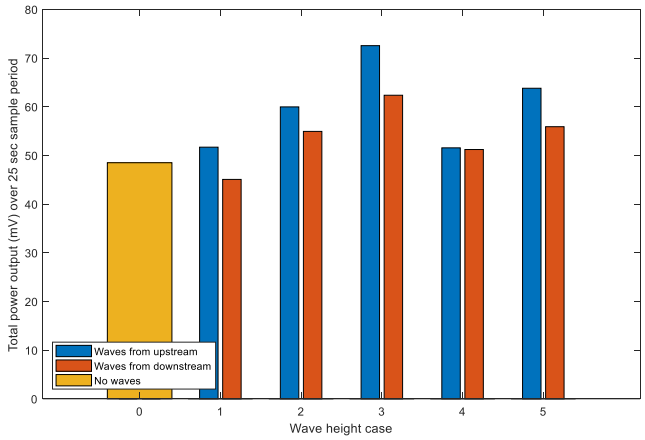

Fig. 5. Turbine power generation over 25-second sample period: Flow cases F2/F5 (1.3m/s) for no waves and wave cases H1-H5.

For each flow case, tests were carried out without waves, and for each of the eight wave cases (two heights with a single period, and two heights with three different periods) described in Table 1. This was also repeated for two direction cases, one where the flow and wave propagation directions were the same, and one where the flow and wave propagation directions were opposing. This gives a total of 18 cases per flow rate, giving an overall total of 72 test cases. However, during initial tests with the 0.8m/s flow case (Messina Strait benign case) it was found that insufficient power was provided to turn the turbine, so this flow case was not used. However, wave heights and periods from this case were still tested with the remaining three flow cases.

III. RESULTS

F. Power generation

Power generation over a 25-second sample period in each test is illustrated in Fig. 5 and Fig. 6. As described previously, data acquisition periods of at least 70 seconds were used, but in some cases with opposing directions of wave propagation and flow, the time taken for the waves to reach the turbine meant that the full data capture period was not representative of the test. In these cases, data for power calculation was taken after the waves had reached the turbine. This resulted in representative periods of around 25 seconds, so this period was adopted for power calculation across all tests.

Results are shown for the middle two flow cases given in Table 1 (i.e. the Messina Strait "Moderate" and "Extreme" cases), with no waves and with five wave height and period combinations: H1, H2, H3, H4 and H5 as shown in Table 2. Flow direction is always from upstream, and results are shown for wave propagation in both the upstream and downstream directions (i.e. in the same direction as, and opposing, the flow).

In all cases with waves, the sample period started after wave action had reached the turbine.

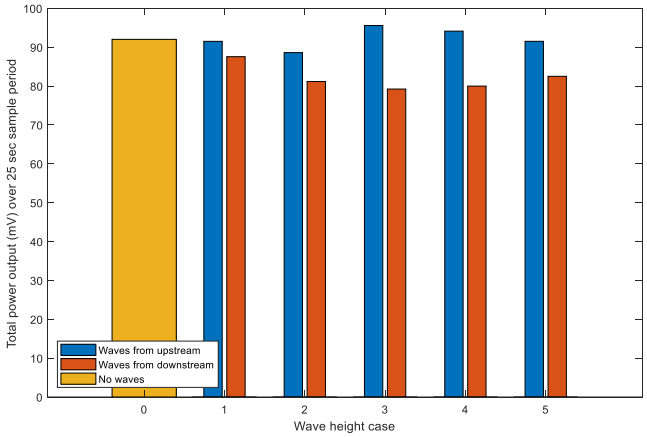

Fig. 6. Turbine power generation over 25-second sample period: Flow cases F3/F6 (1.7m/s) for no waves and wave cases H1-H5.

When waves propagate in the same direction as the flow, total generated power is greater than when waves propagate against the flow. In both flow cases F2 and F3, the greatest power was generated when H3 waves arrived from upstream. The influence of waves appears to be greater in the lower flow rate case, due to the relatively greater ratio of wave energy to flow energy in this case.

Power generation over four wave cycles is shown in Fig. 7 and Fig. 8.

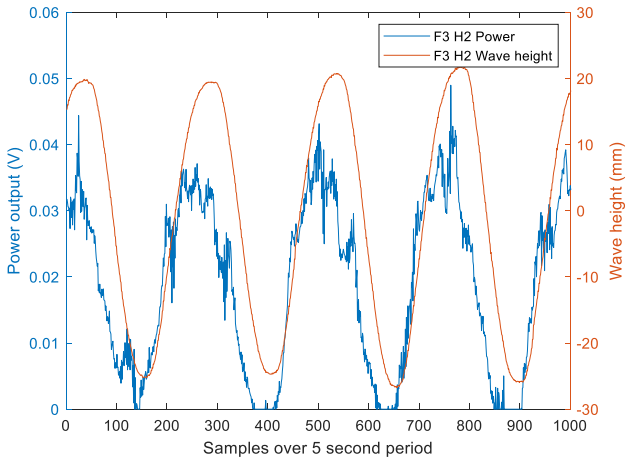

Fig. 7. Turbine power generation and measured wave height over 5-second sample period: Waves from upstream. Flow case 3 (1.7m/s at full scale, 0.19m/s at laboratory scale), wave case H2 (4.0m, 9.0s at full scale, 0.05m, 1.0s at laboratory scale).

As shown in the first figure, when waves and flow direction agree, turbine power output follows the pattern of the waves, with the greatest turbine power output occurring during as the peak of the wave passes over the turbine. Fig. 8 shows the case where waves arrive from downstream turbine, while flow arrives from upstream. This results in a different location of the maximum power point, which this time occurs at the wave minima and falls then rises as the wave passes the turbine.

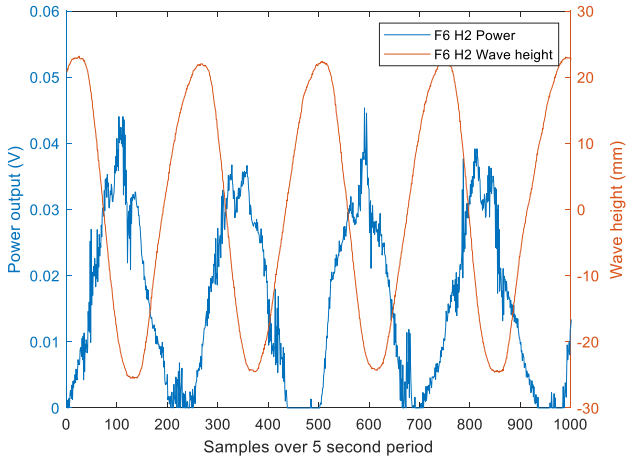

Fig. 8. Turbine power generation and measured wave height over 5-second sample period: Waves from downstream. Flow case 6 (1.7m/s at full scale, 0.19m/s at laboratory scale), wave case H2 (4.0m, 9.0s at full scale, 0.05m, 1.0s at laboratory scale).

G. *Structural deflection*

Structural deflection was recorded using strain gauges, as described in earlier sections. Data from the strain gauge translated to applied force on the support structure is presented in Fig. 9 and Fig. 10, for waves from upstream and downstream respectively.

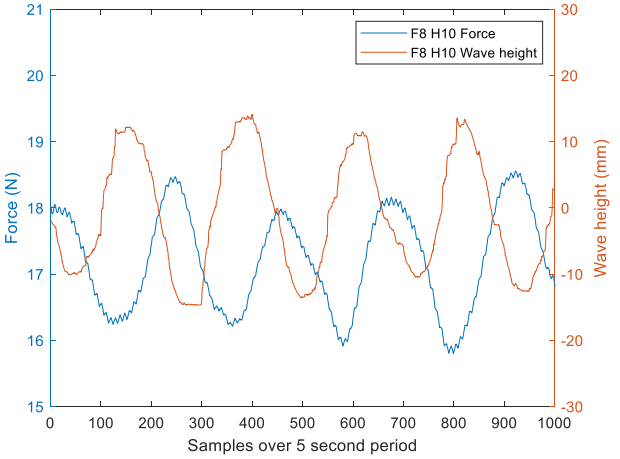

Fig. 9. Force acting on turbine support structure and measured wave height over 5-second sample period: Waves from upstream. Flow rate 2.1m/s at full scale (0.23m/s at laboratory scale), wave case H10 (5.7m/9.0s at full scale, 0.07m/1.0s at laboratory scale.

Relative to wave height, it can be seen that in the case of waves arriving from upstream, the maximum deflection of the turbine support structure occurs just before the wave minima. In the case of waves arriving from downstream, the peak deflection is at the wave maxima. However, in the case of waves from downstream, the range of support structure deflection is greater than that observed when waves arrive from upstream. Similarly, measured wave height is smaller in the case of waves from upstream.

This confirms our assumption that the greatest structural deflection would occur in the case of wave propagation and flow from the same direction.

IV. DISCUSSION

H. *Case comparison: Normalised power coefficient*

In order to compare turbine power output across the range of flow rates tested, results were compared in terms of normalised power coefficient. Results from all cases tested are shown in Fig. 11.

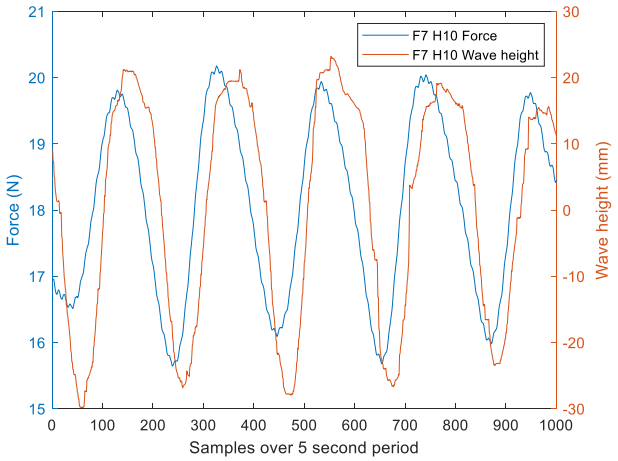

Fig. 10. Force acting on turbine support structure and measured wave height over 5-second sample period: Waves from downstream. Flow rate 2.1m/s at full scale (0.23m/s at laboratory scale), wave case H10 (5.7m/9.0s at full scale, 0.07m/1.0s at laboratory scale).

In cases F2, F3 and F7, waves are from upstream, i.e. the flow and wave propagation direction are the same. In cases F5, F6 and F8 waves arrive from downstream, i.e. the directions are opposing.

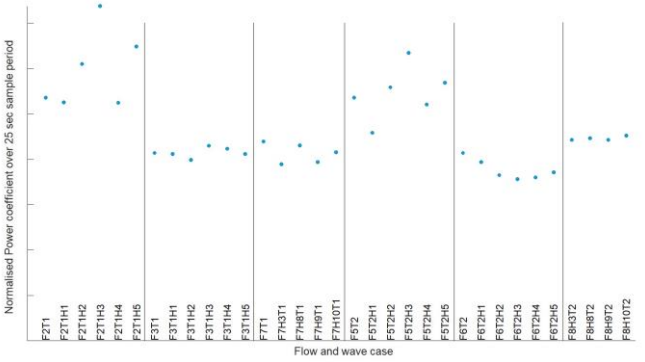

Fig. 11. Normalised power coefficient for flow and wave cases as described in Table 1 (F1/F4 excluded as described previously).

In Fig. 11, it can be seen that the greatest power coefficients are generated under low flow rate cases (F2

and F5). These cases simulate real flow cases of 1.3m/s, representing the MS moderate case and the IS benign case. Within these flow cases, a clear pattern can also be observed in the variation of Cp with wave case. In both cases, the H3 wave case results in the greatest Cp values, and the H1 wave case results in the lowest Cp values. The H3 wave case is the largest wave height simulated, with the longest period (simulating a 5.7m wave with a 10.8s period).

From these results, we suggest that at low flow rates, waves can actually have a positive impact on total power generation, and that the superposition of waves and flow is part of the reason for the increased power coefficients in this cases. However, this is only part of the story, since the effect of the waves on the forces acting on the support structure of the turbine should also be considered.

I. Case comparison: Power vs force

One of the aims of this work is to discover any correlation between the force applied to the support structure and the power generated by the turbine. In order to determine whether such a correlation exists, the total 25-second period power generation in each case was compared to the maximum range of force experienced by the support structure during the same period (i.e. the greatest difference between subsequent force minima and maxima). The method focusses on the force applied to the support structure by the waves as opposed to that applied by the flow, but we believe this is reasonable since

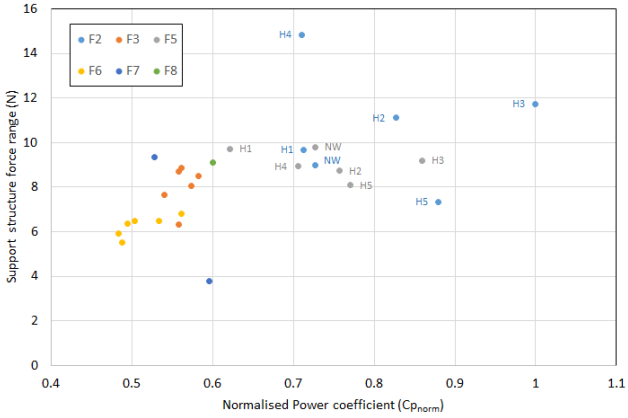

Fig. 12. Normalised power coefficient (Cp_{norm}) vs support structure force range (N) for cases F2, F3, F5, F6, F7, F8.

structural damage caused to the turbine is likely to be caused by fatigue damage due to loading cycles.

This data is shown in Fig. 12.

As in Fig. 11, the F2 and F5 cases exhibit the greatest power coefficient values. For the ease of reading, individual case labels are given for these cases only. Comparing these values to the structural force range, three points in the F2 case demonstrate particularly high values of structural forces. These are the F2H4 (Cp_{norm}=0.72), F2H2 (Cp_{norm}=0.83) and F2H3 (Cp_{norm}=1.0). The loading forces measured over a 25-second sample period for the F2H4 case are shown in Fig. 13.

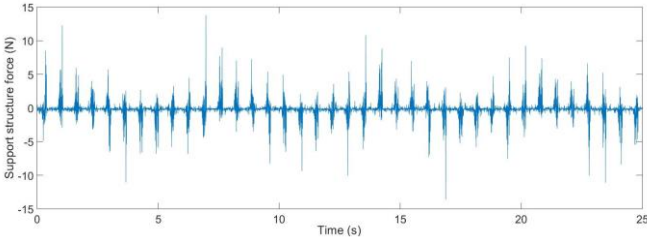

Fig. 13. Support structure measured force for F2H4 case over 25 second sample period.

Fig. 12 also suggests that some flow cases will always deliver lower than average power results, regardless of wave case. The F3 and F6 cases appear to fall into this category.

V. CONCLUSIONS

- Over the action of a single wave, the direction of the wave impacts the point in time at which maximum power is generated. Waves from upstream result in maximum power being generated as the wave crest passes the turbine, but waves from downstream result in maximum power generation at the passing of the wave minima.
- Over a sufficiently long period of time, the direction of wave action appears to have little effect on total power generation of a turbine.
- In some low flow velocity cases, wave action appears to actually improve overall turbine power generation. In the cases we tested, the maximum power was generated by simulating a 5.7m wave with a 10.8s period passing the turbine when placed in a flow rate of 1.3m/s.
- In the Messina Strait environment, this represents a moderate flow rate with an extreme wave case. In the Sound of Islay case this represents a benign flow rate with a moderate wave case.

Further analysis of these results is required to study detailed hydrodynamic effects and to ascertain the exact mechanism through which the wave affects the turbine and why it does so differently in these particular flow cases. As noted above, cases F3 and F6 result in lower power coefficient values than F7 and F8 cases. Further tests on a greater range of cases between the flow velocities of these cases (i.e. between velocities of 1.7m/s and 2.1m/s) may reveal interesting results.

Ultimately, it is also hoped that the results of these tests will be used to create a lifetime fatigue model of a turbine, which can be used to consider the lifetime balance of power generation and structural impacts. This is an interesting area of work since the acceptability of structural forces in comparison with power generation will vary on a site-by-site basis, as well as by infrastructure owner.

REFERENCES

[1] E.E. Lust, L. Luznik, K.A. Flack, J.M. Walker, M.C. Van Benthem. "The influence of surface gravity waves on marine current turbine performance", *International Journal of Marine Energy*, vol. 3–4,pp. 27-40, 2013. ISSN: 2214-1669, [Online]. Available: https://doi.org/10.1016/j.ijome.2013.11.003.

[2] S.C. Tatum, C.H. Frost, M. Allmark, D.M. O'Doherty, A. Mason-Jones, P.W. Prickett, R.I. Grosvenor, C.B. Byrne, T. O'Doherty. "Wave–current interaction effects on tidal stream turbine performance and loading characteristics", *International Journal of Marine Energy*, vol. 14, 2016, pp. 161-179, 2016, ISSN: 2214-1669, [Online]. Available: https://doi.org/10.1016/j.ijome.2015.09.002.

[3] S. Draycott, G. Payne, J. Steynor, A. Nambiar, B. Sellar, V. Venugopal. "An experimental investigation into non-linear wave loading on horizontal axis tidal turbines". *Journal of Fluids and Structures*, vol. 84. pp. 199-217, 2019. ISSN: 0889-9746.

[4] S. Draycott, A. Nambiar, B. Sellar, T. Davey, V. Venugopal. "Assessing extreme loads on a tidal turbine using focused wave groups in energetic currents", *Renewable Energy*, vol. 135, pp. 1013-1024, 2019. [Online]. Available: https://doi.org/10.1016/j.renene.2018.12.075.

[5] Cucco, A., Quattrocchi, G., Olita, A., Fazioli, L., Ribotti, A., Sinerchia, M., Tedesco, C., Sorgente, R. "Hydrodynamic modelling of coastal seas: the role of tidal dynamics in the Messina Strait, Western Mediterranean Sea", *Nat. Hazards Earth Syst. Sci*. vol. 16, pp. 1553–1569, 2016.

[6] Sergio G. Longhitano. "Between Scylla and Charybdis (part 1): the sedimentary dynamics of the modern Messina Strait (central Mediterranean) as analogue to interpret the past", *Earth-Science Reviews* vol. 185, pp. 259-287, 2018.

[7] A. Copping, "Sound of Islay Demonstration Tidal Array," Tethys, Pacific Northwest National Laboratory, 4th February 2019. [Online] Available: https://tethys.pnnl.gov/annex-iv-sites/sound-islay-demonstration-tidal-array

[8] Bathymetric metadata and Digital Terrain Model data , EMODnet Bathymetry portal, 9th October 2018, [Online] Available: http://www.emodnet-bathymetry.eu

[9] E.U. Copernicus Marine Service Information: Copernicus Environment Monitoring Service Global Ocean 1/12° Physics Analysis and Forecast. Product GLOBAL_ANALYSIS_FORECAST_PHY_001_024. Longitude -8 to -1, latitude 55 to 59. Date 01/01/2017 00:30:00 to 31/21/2017 23:30:00

[10] E.U. Copernicus Marine Service Information: Copernicus Environment Monitoring Service Global Ocean 1/12° Physics Analysis and Forecast. Product GLOBAL_ANALYSIS_FORECAST_PHY_001_024. Longitude 14 to 17, latitude 36 to 39. Date 01/01/2017 00:30:00 to 31/21/2017 23:30:00

[11] D. Vicinanza, L. Cappietti, P. Contestabile, 2009. "Assessment of Wave Energy around Italy". *Proceedings of the 8th European Wave and Tidal Energy Conference*, Uppsala, Sweden, 2009.

[12] Pelli, D., Cappietti, L., Oumeraci, H. "Assessing the wave energy potential in the Mediterranean Sea using WAVEWATCH III". *Proceedings of Renew 2016, 2nd International Conference on Renewable Energies Offshore*, 2016.

[13] DHI MetOcean Data Portal. Global Wind Speed, Wave Height and Wave Period, Satellite Altimeter Measurements. Geographical reference EPSG:4326 (WGS84). NASA Jason-1 satellite data via MetOcean Data Portal for 15/3/16 - 15/3/17.

[14] T. Blackmore, W.M.J. Batten, A.S. Bahaj, "Influence of turbulence on the wake of a marine current turbine simulator", *Philos. Trans. Royal Soci*. vol. 470, no. 2170, 2014. [Online]. Available: https://doi.org/10.1098/rspa.2014.0331.

[15] T. Blackmore, L.E. Myers, A.S. Bahaj. "Effects of turbulence on tidal turbines: Implications to performance, blade loads, and condition monitoring", *International Journal of Marine Energy*, vol. 14, 2016, pp. 1-26, 2016. ISSN 2214-1669.

[16] Ahmadi, M. "Influence of upstream turbulence on the wake characteristics of a tidal stream turbine", *Renewable Energy*, vol. 132, pp. 989-997, 2019. ISSN 0960-1481.

[17] S. Walker, L. Cappietti, "Experimental Studies of Turbulent Intensity around a Tidal Turbine Support Structure", *Energies*, vol. 10, no. 497, 2017.

[18] Milne I., Sharma R., Flay R., Bickerton S. "Characteristics of the turbulence in the flow at a tidal stream power site", *Philos Trans A Math Phys Eng Sci.* vol. 371, no. 1985, 2013. DOI: 10.1098/rsta.2012.0196.